Cell, Vol. 119, 407–418, October 29, 2004, Copyright ©2004 by Cell Press

Structural Mechanism for Lipid Activation of the Rac-Specific GAP, β2-Chimaerin

Bertram Canagarajah,[1] Federico Coluccio Leskow,[2] Jonathan Yew Seng Ho,[1,3,4] Harald Mischak,[1,3,5] Layla F. Saidi,[1,3] Marcelo G. Kazanietz,[2] and James H. Hurley[1,*]

[1]Laboratory of Molecular Biology
National Institute of Diabetes and Digestive and Kidney Diseases
National Institutes of Health
U.S. Department of Health and Human Services
Bethesda, Maryland 20892

[2]Department of Pharmacology and Center for Experimental Therapeutics
University of Pennsylvania School of Medicine
Philadelphia, Pennsylvania 19104

Summary

The lipid second messenger diacylglycerol acts by binding to the C1 domains of target proteins, which translocate to cell membranes and are allosterically activated. Here we report the crystal structure at 3.2 Å resolution of one such protein, β2-chimaerin, a GTPase-activating protein for the small GTPase Rac, in its inactive conformation. The structure shows that in the inactive state, the N terminus of β2-chimaerin protrudes into the active site of the RacGAP domain, sterically blocking Rac binding. The diacylglycerol and phospholipid membrane binding site on the C1 domain is buried by contacts with the four different regions of β2-chimaerin: the N terminus, SH2 domain, RacGAP domain, and the linker between the SH2 and C1 domains. Phospholipid binding to the C1 domain triggers the cooperative dissociation of these interactions, allowing the N terminus to move out of the active site and thereby activating the enzyme.

Introduction

Diacylglycerol is a paradigmatic lipid second messenger in metazoan cell signaling, the first to be discovered (Kikkawa et al., 1989; Nishizuka, 1988, 1992, 1995). Diacylglycerol is a central mediator of downstream signaling by a host of hormones coupled through G_q and phospholipase C-β, growth factors coupled to tyrosine kinase-linked receptors and phospholipase C-γ, and many other extra- and intracellular stimuli (Nishizuka, 1995). The protein kinase C (PKC) isozyme family has historically been the most intensively studied class of targets for diacylglycerol signaling (Kikkawa et al., 1989; Mellor and Parker, 1998; Newton and Johnson, 1998; Nishizuka, 1988, 1992, 1995; Ron and Kazanietz, 1999). In response to diacylglycerol, conventional and novel PKC isozymes, and the protein kinase D isozymes, translocate to membranes, where they phosphorylate Ser and Thr residues in diverse proteins. The diacylglycerol-responsive PKC isozymes are also activated by phorbol esters, which are potent agonists that bind to the same site as diacylglycerol. These PKC isozymes are activated by diacylglycerol and phorbol esters by virtue of their direct binding to motifs known as protein kinase C homology-1 (C1) domains (Hurley et al., 1997; Newton and Johnson, 1998; Nishizuka, 1992, 1995; Ono et al., 1989; Ron and Kazanietz, 1999).

In recent years, it has become clear that there are several major classes of C1 domain-containing diacylglycerol receptors in addition to PKC. Munc-13 proteins are phorbol ester binding scaffolding proteins involved in Ca^{2+}-stimulated exocytosis (Betz et al., 1998; Brose and Rosenmund, 2002; Rhee et al., 2002). RasGRPs are diacylglycerol-activated guanine-nucleotide exchange factors (GEFs) for Ras and Rap1 (Ebinu et al., 1998; Tognon et al., 1998). The α- and β-chimaerins are a family of phorbol ester- and diacylglycerol-responsive GTPase-activating proteins (Ahmed et al., 1990, 1993; Areces et al., 1994; Caloca et al., 1997, 1999; Hall et al., 1990; Leung et al., 1994).

In vitro studies using recombinant chimaerin isoforms show that, like PKCs, they bind phorbol esters with low nanomolar affinity in the presence of acidic phospholipids (Areces et al., 1994; Caloca et al., 1997). α1-chimaerin (formerly known as *n*-chimaerin) and α2-chimaerin are alternatively spliced products of a single gene, as are β1- and β2-chimaerin. β2-chimaerin contains three conserved domains. The N-terminal Src homology-2 (SH2) domain is presumed competent to bind phosphotyrosine-containing proteins, but its physiological partner is unknown. The central C1 domain is followed by a C-terminal GAP domain with homology to many other Rho, Rac, and Cdc42 GAPs. The GAP activity of β2-chimaerin is specific for Rac as opposed to other small G proteins (Caloca et al., 2003). Rac is a member of the Rho small GTP binding protein (G protein) family that also includes Rho and Cdc42 isoforms. These small G proteins regulate actin dynamics, transcription, the cell cycle, cell adhesion, and many other cell processes (Bishop and Hall, 2000). The proper function of GAPs in cell regulation is vitally important since failure to appropriately inactivate small G proteins is associated with cancer (Bishop and Hall, 2000). Indeed, downregulation of β2-chimaerin has been found in some types of cancers such as high-grade gliomas, and the reduced expression of this gene may contribute to the development of the tumor (Yuan et al., 1995).

C1 domains are compact zinc fingers of 50–51 amino acids. Their structure comprises two small β sheets and a single helix folded around two Zn^{2+} ions (Hommel et al., 1994; Hurley and Misra, 2000; Hurley et al., 1997; Zhang et al., 1995). The two strands in the smaller β sheet are pulled apart, due to a break in their hydrogen bonding induced by a conserved Pro residue. Phorbol ester binds stereospecifically in the groove formed

*Correspondence: hurley@helix.nih.gov

[3]These authors contributed equally to this work.

[4]Present address: Prolexys Pharmaceuticals, Salt Lake City, Utah 84116.

[5]Present address: Department of Nephrology, Medizinische Hochschule Hannover and Mosaiques Diagnostics AG, Feodor-Lynen Str. 21, 30625 Hannover, Germany.

where the two strands pull away from each other. The stereospecific phorbol ester binding site is surrounded on three sides by bulky hydrophobic side chains, which form a hydrophobic wall around the phorbol ester binding site (Zhang et al., 1995). Distal to the phorbol ester binding site, Arg, Lys, and His residues form a basic belt on the surface of the C1 domain. The hydrophobic wall inserts in the hydrocarbon core of phospholipid bilayers upon binding, while the basic belt interacts with acidic phospholipid headgroups (Xu et al., 1997a). The high affinity of C1 domain/phorbol ester interactions in the presence of bilayers or micelles is due to the synergism between the stereospecific phorbol ester binding and nonspecific binding of acidic phospholipids to the basic and hydrophobic exterior surface of the C1 domain (Kazanietz et al., 1995a). Translocation and activation of C1 domain proteins requires the interplay of specific and nonspecific activators: both diacylglycerol or phorbol ester and bulk phospholipid.

Structural and functional studies of C1 domains have established the mechanism for diacylglycerol and phorbol ester-induced translocation to membranes (reviewed in Hurley and Meyer [2001]; Hurley and Misra [2000]; Newton and Johnson [1998]). Concomitant with membrane translocation, PKCs, chimaerins, and other C1 domain proteins become allosterically activated. The PKC activation mechanism is thought to require a large conformational change, on the basis of changes in susceptibility to limited proteolysis (Orr et al., 1992; Orr and Newton, 1994), translocation kinetics (Oancea and Meyer, 1998), fluorescence (Slater et al., 1999), surface pressure analysis (Medkova and Cho, 1999), and other indirect structural techniques. In the absence of direct structural information on an intact C1 domain-containing protein, the nature of such conformational changes has been elusive. Here we report the crystal structure of full-length β2-chimaerin and deduce a mechanism for its allosteric activation by lipids.

Results

β2-chimaerin was expressed as a recombinant protein using the baculovirus/Sf9 cell system, purified, and crystallized. The structure of β2-chimaerin was determined by single anomalous dispersion from the two native Zn^{2+} ions and a single Xe atom, in combination with molecular replacement, using the SH2 domain of Src (Xu et al., 1997b), the C1B domain of PKCδ (Zhang et al., 1995), and the RhoGAP domain of Cdc42GAP (Nassar et al., 1998) as probes. The structure has been refined to an R factor of 0.25 at a resolution of 3.18 Å (Table 1). The entire sequence can be visualized in the electron density (Figure 1A), with the exception of the first 20 residues and residues 162–208 from the SH2-C1 domain linker. The domains are arranged with the C1 domain in the middle and the RacGAP and SH2 domains on either side (Figure 1B). The overall dimensions of the structure are 85 × 55 × 40 Å.

SH2 Domain

The SH2 domain is superimposable on the structures of other such domains. The rmsd (for Cα positions, excluding the last helix) versus the SH2 domain of Src (Xu et al., 1997b) is 1.5 Å. The most notable feature of the SH2 domain is that the C-terminal (αB) helix is longer, five turns as compared to three in Src and its relatives (Sicheri et al., 1997; Xu et al., 1997b), and the helix is in a different orientation (Figure 1C). The final strand, βG, which follows the αB helix in canonical SH2 domains, is absent. The SH2 domain resembles that of the APS adaptor protein, which also has a long αB helix and lacks the βG strand (Hu et al., 2003). The side chains of Arg64, Arg81, and Arg104, and the main chain NH group of Gln84 together form an apparent pocket for phosphotyrosine binding. However, in the uncomplexed structure observed here, the side chain of Arg64 is rotated away from the phosphotyrosine binding site.

C1 Domain

The C1 domain is at the heart of the tertiary structure of β2-chimaerin. The C1 domain is closely superimposable on the C1B domain of PKC-δ, with an rmsd (all Cα positions) of 0.8 Å (Figure 1D). The C1 domain makes extensive contacts with the N terminus, both the SH2 and RacGAP domains, and with interdomain linkers. The C1 domain has a total of 4056 $Å^2$ of solvent-accessible surface area in isolation; this is reduced to 2481 $Å^2$ in intact β2-chimaerin. The putative membrane binding basic residues on the C1 surface (Lys216, His218, Arg221, His224, Arg242, and Lys252) are solvent exposed. The putative membrane binding hydrophobic residues Pro223, Trp225, Phe232, and Trp234 are completely buried in intramolecular contacts with the rest of β2-chimaerin (Figure 2A). Leu236 and Ile237 are partially buried in contacts with the SH2 domain. The polar surface of the C1 domain is for the most part solvent exposed. Among the exceptions is Asn231, which forms a hydrogen bond with Tyr141 of the SH2-C1 linker. Tyr228 forms hydrophobic contacts with Pro149 and Tyr151 of the SH2-C1 linker.

RacGAP Domain

The RacGAP domain is homologous to the structurally characterized RhoGAP domains of p120GAP (Scheffzek et al., 1996), PI 3-kinase p85α subunit (Musacchio et al., 1996), p50RhoGAP (Rittinger et al., 1997a; Rittinger et al., 1997b), and Cdc42GAP (Nassar et al., 1998). The structures are similar, as expected from sequence similarity (Figure 1E). The RacGAP domain of β2-chimaerin can be superimposed on the RhoGAP domains of p50RhoGAP (Rittinger et al., 1997b) and Cdc42GAP (Nassar et al., 1998) with rmsd values of 1.2 Å for both. The β2-chimaerin RacGAP domain structure has no major differences with the unliganded structure of the RhoGAP domain of p50RhoGAP (Barrett et al., 1997). The largest change between the β2-chimaerin RacGAP domain and the RhoGAP domain in the p50RhoGAP/RhoA-GDP·AlF_x^- complex structure of RhoGAP domains (Rittinger et al., 1997b) is seen in the αF′ helix, which moves 6 Å to bind to the small G protein in the bound form (Figure 1E).

No experimental structure of the RacGDP·AlF_x^- complex with β2-chimaerin is available, so this structure was modeled by superimposing the RhoGAP domain of the p50RhoGAP/RhoA-GDP·AlF_x^- complex on the β2-chimaerin RacGAP domain. The structure of RacGDP·AlF_x^-

Table 1. Crystallographic Data Collection, Phasing, and Refinement Statistics

(A) Crystallographic Data and Phasing Statistics

Space group:		$P6_122$			
Cell dimensions (Å), native:		a = b = 131.28, c = 289.04, α = β = 90°, γ = 120°			
Cell dimensions (Å), xenon derivative:		a = b = 131.07, c = 284.70, α = β = 90°, γ = 120°			
	dmin (Å)	No. of reflections	Completeness (%)[a]	$\langle I \rangle / \langle \sigma \rangle$[a]	Rsym (%)[a,b]
Native (λ = 1.1 Å)	3.2	109,671	99.5 (98.8)	27.0 (3.3)	5.8 (58.0)
Xenon (λ = 1.28 Å)	3.8	244,997	95.0 (69.1)	34.5 (3.8)	7.9 (49.6)

Phasing

Bijvoet ratio[c], Xe, λ = 1.28: 4.5%	
Figure of merit: 0.29 (0.66)[d]	
Phasing power: 1.30	

(B) Refinement

Resolution range	20.0 – 3.2 Å
Number of reflections	23,767
$R_{working}$[e]	24.8%
R_{free}[f]	29.0%
Bond-length deviation	0.008 Å
Bond-angle deviation	1.56°
Average B factor	93.4 Å^2

[a] Values in parentheses are for the highest resolution bin.
[b] $Rsym = \Sigma_h \Sigma_i |I_i(h) - \langle I(h) \rangle| / \Sigma_h \Sigma_i I_i(h)$
[c] Ratio is calculated as $\Sigma \langle |\Delta F| \rangle / \langle |F| \rangle$.
[d] Value in parentheses is the figure of merit after solvent flattening.
[e] $R = \Sigma(||F_{obs}| - k|F_{calc}||)/\Sigma|F_{obs}|$.
[f] R_{free} is the R value calculated for a test set of reflections, comprising a randomly selected 5% of the data that is not used during refinement.

as observed in complex with the GAP domain of *Pseudomonas aeruginosa* ExoS protein was then superimposed on the RhoA portion of the p50RhoGAP/RhoA-GDP·AlF_x^- structure (Wurtele et al., 2001). The modeled β2-chimaerin/Rac complex places Arg311 of β2-chimaerin within 1.9 Å of the nearest F^- ion in the RacGDP·AlF_x^- complex (Figure 3). Most contacts between p50RhoGAP and RhoA on the one hand, and β2-chimaerin and Rac on the other, are conserved. The only major exception is in the RacGAP A′ helix. Phe315 and Glu317 of β2-chimaerin interact with Ala88 and Ala95 of Rac. In Rho, these two Ala are replaced by Asp90 and Glu97, while in p50RhoGAP the Phe and Glu of the RacGAP domain are replaced by Asn and Gln. In another difference, part of the Rac interaction surface on the RacGAP domain is occluded by Pro21 and Pro22 of the N terminus of β2-chimaerin.

N-Terminal and Linker Regions

The ordered part of the N-terminal region of β2-chimaerin (residues 21–54) extends 60 Å, essentially the entire length of the protein (Figure 1F). The segment comprising residues 21–24 is in contact with the RacGAP domain. Residues 27–34 form a helix (αN) that rests against the membrane binding site and covers the phorbol ester binding groove of the C1 domain. Gln32 of the N terminus protrudes into the phorbol ester binding site and forms hydrogen bonds with the unpaired β strand at Gly235 (Figures 2C and 2D). The remaining residues of the N terminus (35–54) form an extended loop reaching to the start of the SH2 domain. Of the first ~25 residues of the SH2-C1 linker, residues 139–147 comprise another helix (αL for "linker") resting on the C1 domain. This αL helix is in contact with and antiparallel to the αN helix.

Mutational Analysis of β2-Chimaerin Translocation and RacGAP Activity

In order to test the role of intramolecular contacts between various domains of β2-chimaerin and the C1 domain, we constructed and characterized ten site-directed mutants of internal contact residues. These residues were selected from positions of the αN and αL helices, and the SH2 and RacGAP domains that contact the C1 domain (Figure 4A). These mutants were designed to destabilize the inactive conformation, thereby lowering the free energy required to reach the active state. To assess the responsiveness to C1 domain ligand binding in a cellular context, we quantitated the translocation of β2-chimaerin in COS-1 cells. Our previous work had shown that β2-chimaerin required a higher concentration of phorbol ester for translocation compared to phorbol ester-responsive PKCs (Caloca et al., 1997, 1999). All but one of the mutants were sensitized to phorbol ester-induced translocation. Remarkably, mutants Q32A-β2-chimaerin and I130A-β2-chimaerin are highly sensitive to PMA-induced translocation, as judged by the significantly lower EC_{50} observed for the phorbol ester effect (Figures 4B and 4C). This last mutant was almost as sensitive as PKCα for PMA-induced translocation. In order to determine whether the mutants had enhanced RacGAP activity in vivo, we directly measured Rac-GTP levels in vivo using a p21 binding domain pull-down assay (Benard et al., 1999). While transfection of wild-type β2-chimaerin reduces Rac-GTP levels by ~25%, the mutants Q32A and I130A reduce Rac-GTP levels by ~40% and 80%, respectively (Figure 5).

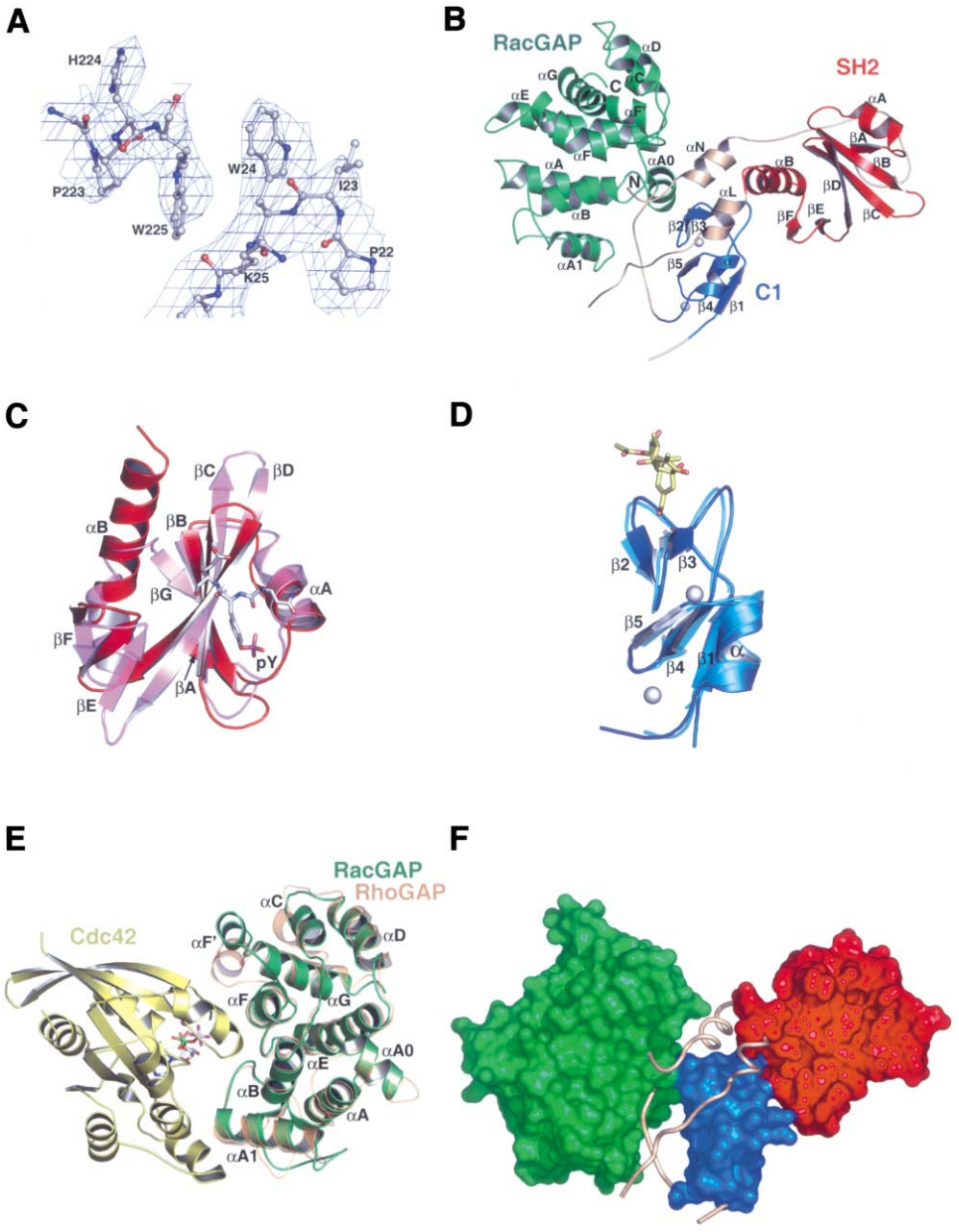

Figure 1. Structure of β2-Chimaerin

(A) Refined model of β2-chimaerin in the vicinity of Gln32 superimposed on the solvent-modified single anomalous dispersion (SAD) Fourier synthesis.

(B) Overall structure of β2-chimaerin. The domains red (SH2), blue (C1), green (RacGAP), and grey (linkers).

(C) Structure of the SH2 domain (red) overlaid on the SH2 domain of Src (cyan) and showing the internal phosphotyrosine-containing sequence in Src in a stick representation.

(D) Structure of the C1 domain (blue) overlaid on the C1B domain of PKCδ (cyan) and showing phorbol ester as bound to the the PKCδ-C1B.

(E) Structure of the RacGAP domain (green) overlaid on the RhoGAP domain of p50RhoGAP (grey), showing the bound Cdc42 protein (yellow) in complex with GDP and AlF_x^- (stick model).

(F) Linker regions are shown in a worm represenation, with the rest of β2-chimaerin shown in a space-filling representation, oriented and colored as in (B).

Discussion

Mechanism of Membrane Translocation

The protein targets of diacylglycerol translocate from the cytosol to membranes in response to diacylglycerol signals or phorbol ester treatment. This translocation is driven by diacylglycerol or phorbol ester binding to the C1 domain, concomitant with C1 domain penetration into the membrane. The crystal structure of the PKCδ C1B domain in complex with phorbol ester showed that exposed hydrophobic side chains ring the bound phorbol ester but make limited or no direct contact with it

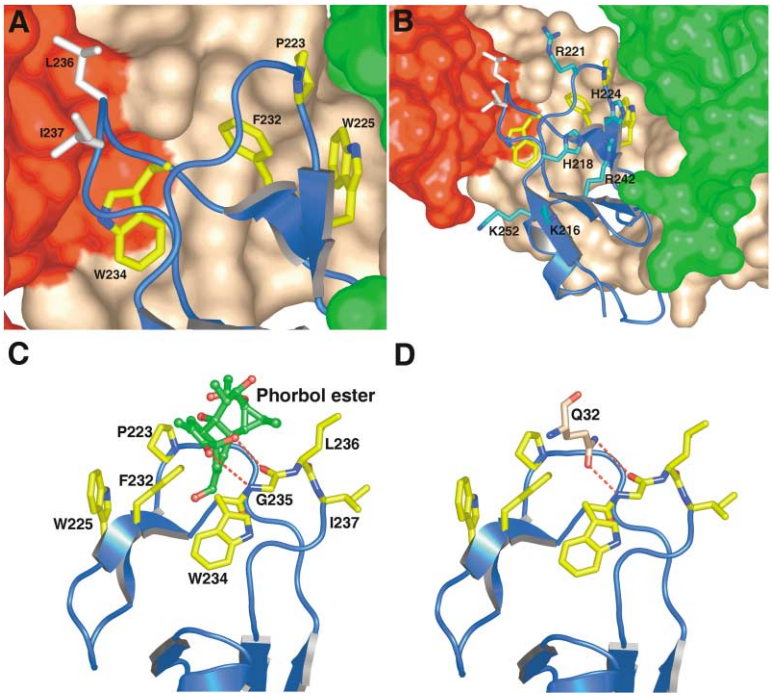

Figure 2. Membrane Insertion and Phorbol Ester Binding Sites on the C1 Domain

(A) Hydrophobic residues on the membrane-inserting rim of the C1 domain. Residues that are completely buried in intramolecular contacts are colored yellow and residues that are partially buried, white. The remainder of β2-chimaerin is shown in a surface representation.

(B) The solvent-exposed environment of the membrane-interacting basic residues (stick model) of the C1 domain is shown.

(C) Docked model of phorbol ester (green) bound to the β2-chimaerin C1 domain, with hydrogen bonds indicated.

(D) The C1 domain and Gln32 from the αN helix are shown.

(Zhang et al., 1995). Five of these side chains are identical or conserved throughout all phorbol ester binding C1 domains (Hurley et al., 1997). In the PKCδ C1B domain, these are Pro231, Phe243, Leu250, Trp252, and Leu254. There are two other prominent exposed hydrophobic side chains nearby on the PKCδ C1B domain, Met239 and Val255, which are incompletely conserved in phorbol ester binding C1 domains. In β2-chimaerin, the Met239 is replaced by Arg223, and the remaining exposed hydrophobic residues are conserved (Figure 2B).

Several lines of evidence show that the hydrophobic ring surrounding the phorbol ester binding site inserts into the membrane. The 12- and 13-positions of the phorbol ester, which are esterified to acyl groups that are membrane bound, point in the same direction as the hydrophobic side chains. Docking of a long chain phorbol ester into the membrane requires that these side chains penetrate the membrane. These residues of PKCδ are critical for phorbol ester binding when the ligand is presented in micelles, as judged by the ablation of binding in site-directed mutants at these positions (Kazanietz et al., 1995b). The NMR structure of the C1B domain of PKCγ determined in the presence of phorbol ester and short chain phospholipid micelles (Xu et al., 1997a) shows that the hydrophobic side chains interact with the phospholipid micelles. Surface pressure analysis of PKCα shows that it penetrates membranes upon diacylglycerol-induced membrane binding (Medkova and Cho, 1999) and that mutations of the hydrophobic side chains in the C1A domain of PKCα block penetration (Medkova and Cho, 1999). The C1 domains of PKCα, γ, and δ, and β2-chimaerin are highly conserved (46% identity between the PKCδ C1B and the β2-chimaerin C1 domain sequences). The membrane penetration studies have been executed on closely related systems, and the results are consistent with a common picture of the translocation mechanism.

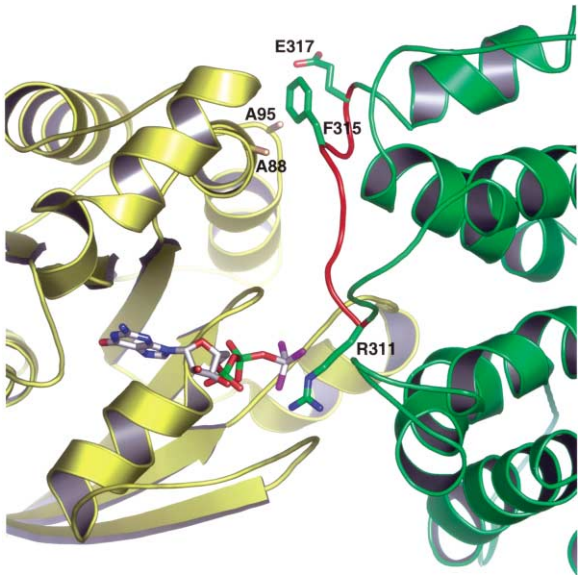

Figure 3. Model of the β2-Chimaerin (green)/Rac (yellow) Complex with GDP and AlF_x^-

The burial of ~40% of the C1 domain surface, and almost all of its presumed membrane insertion site, is a key observation in this study. The C1 domain surfaces buried in these contacts overlap extensively with the surfaces involved in phospholipid and phorbol ester binding. Of the six hydrophobic side chains believed to insert into the membrane, four are completely buried, and two are partially buried in contacts with the rest of the protein. The main chain NH and CO groups on Gly235 are presumed to interact with the 3- and 4-hydroxyls

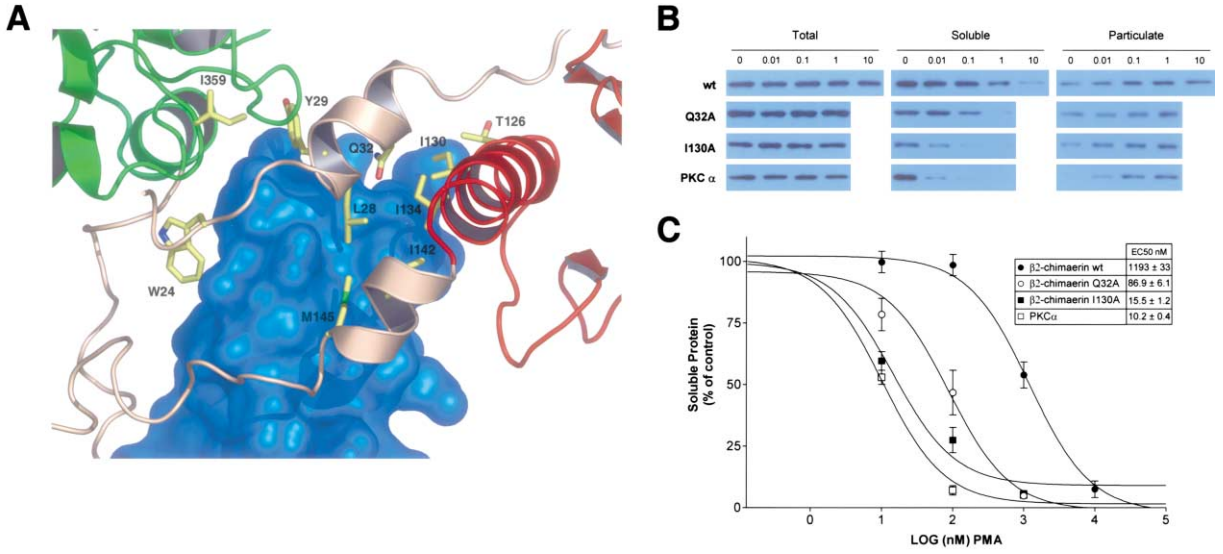

D

Protein	β2-chim	β1-chim	W24A	L28A	Y29A	Q32A	T126A	I130A	I134A	I142A	M145A	I359A	PKC α
EC50	1193 ± 33	20.19 ± 0.9	20.7± 3.2	14.7 ± 2.5	58.5 ± 3.6	86.9 ± 6.1	4902 ± 342	15.5 ± 1.2	50.8 ± 5.7	54.1 ± 5.0	66.2 ± 8.1	45.6 ± 5.3	10.2 ± 0.4

Figure 4. β2-Chimaerin Translocation in Cells

(A) Residues targeted for mutational analysis. Domains of β2-chimaerin are colored as in Figure 1.

(B and C) COS-1 cells were transfected with pEGFP-β2-chimaerin (wild-type), pEGFP-β2-chimaerin-Q32A, or pEGFP-β2-chimaerin-I130A. Forty-eight hours later, cells were incubated with different concentrations of PMA for 20 min and subjected to subcellular fractionation. Representative Western blots using an anti-GFP antibody or for endogenous PKCα are shown in (B). Panel C shows a densitometric analysis of the immunoreactivity in the soluble fraction. Results are expressed as percentage of the values observed in control (nontreated) cells and represent the mean standard error of 4–7 independent experiments. The corresponding EC_{50} values are shown in the inset.

(D) EC_{50} values for all ten mutants constructed.

of phorbol ester, as seen for Gly253 of PKC-δ. In β2-chimaerin, the amide group of the side chain of Gln32 replaces this interaction and sterically blocks the phorbol ester binding site. This implies that the observed conformation of β2-chimaerin is incompatible with phorbol ester and phospholipid membrane binding. Four different regions of the protein contact the C1 domain: the N terminus, the SH2 domain, the SH2-C1 linker, and the RacGAP domain. These four different regions converge at the membrane insertion site on the C1 domain, and each of the four is directly involved in contacts with the hydrophobic side chains.

The cost in free energy to break the extensive interactions between the C1 domain and these four protein regions must be considerable. This would lead to the prediction that intact β2-chimaerin would translocate to membranes at higher doses of phorbol ester than required for the C1 domain alone or for proteins with less buried C1 domains. Indeed, β2-chimaerin translocation to cell membranes requires a dose ~100-fold higher than translocation of PKCα (Caloca et al., 2001). β1-chimaerin, the product of alternative splicing of the same gene as β2-chimaerin, lacks the SH2 domain of β2-chimaerin and therefore has fewer intramolecular interactions with the C1 domain. β1-chimaerin translocates to membranes at a much lower dose of phorbol ester than β2-chimaerin, consistent with a greater degree of solvent exposure of its C1 domain (Figure 4D).

In order to directly test the concept that intramolecular interactions with specific regions within β2-chimaerin inhibit membrane binding, and therefore phorbol ester-induced translocation, ten single-site mutants were constructed in each of the four regions of β2-chimaerin that interact with the C1 domain. Nine of the ten mutants decrease the EC_{50} for phorbol ester-induced translocation, with the sensitization ranging from 15- to 90-fold. The smallest enhancement, 15-fold, is seen in the Q32A mutant, which obliterates polar interactions, rather than the hydrophobic interactions lost in other mutants. The largest enhancements of phorbol ester sensitivity, 90-fold, are seen in the mutants L28A and I130A. Leu28 buries itself against the junction between αL and the C1 domain, while Ile130 is buried in the αN/C1 interface. Mutating residues that stabilize more than one interdomain contact thus produces the largest sensitivity enhancements. One mutation, T126A, produces an effect opposite to the rest, increasing the phorbol ester EC_{50} by 4-fold. Thr126 has a 3.4 Å close contact with Leu236 of the C1 domain, and this contact appears to push Leu236 into a less favorable conformation than that observed in the PKCδ-C1B structure. The T126A mutant may relieve intramolecular steric strain, thereby stabilizing the inactive conformation of β2-chimaerin.

We infer from this structure that the cooperative collapse of all of these interactions is a prerequisite for membrane binding. In other words, membrane binding by β2-chimaerin must be coupled to a massive conformational change involving the entire protein. We mod-

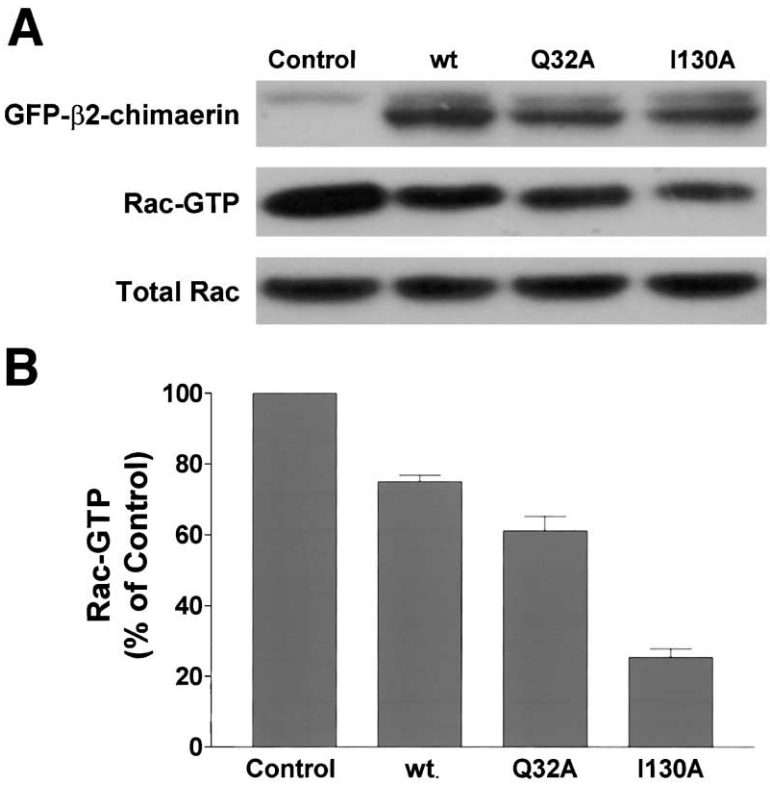

Figure 5. RacGAP Activation in Cells

Rac-GTP levels were measured in COS-1 cells untransfected (control) or transfected with plasmids encoding for GFP-β2-chimaerin wild-type (wt), Q32A or I130A. After transfection, cells were grown in full medium for 48 hr.

(A) Representative experiment showing Rac-GTP levels, total Rac levels, and the expression of the corresponding GFP-fusion proteins.

(B) Densitometric analysis of Rac-GTP levels normalized to total Rac levels in each case. Values are expressed as % of control and they represent the mean of seven independent experiments ± SE. Differences between groups are significant by t test with $p < 0.001$, except wt versus Q32A ($p < 0.036$).

eled the structure of the active, membrane bound conformation (Figure 6) based on the assumption that hydrophobic surfaces liberated by the collapse of interdomain interactions would preferentially embed themselves in the surface of the membrane, rather than remaining exposed to aqueous solvent.

Mechanism of Rac Recognition, Specificity, and GTPase Activation

The β2-chimaerin structure, taken together with modeling of the β2-chimaerin/Rac transition state-like complex, shows how β2-chimaerin could promote the GTPase activity of Rac. Based on the model, Arg311 of β2-chimaerin acts as the "arginine finger," reaches into the active site of Rac, and directly stabilizes the transition state for GTP hydrolysis. The structure explains the specificity of β2-chimaerin for Rac, as opposed to its close relatives Rho and Cdc42. In a hypothetical β2-chimaerin/Rho complex, unfavorable steric and electrostatic interactions would be formed between the Asp90 and Glu97 of Rho and the Phe315 and Glu317 of β2-chimaerin. These interactions should be particularly disruptive to catalysis, given their proximity to the catalytic Arg311. Asp90 of RhoA has been shown to be a key determinant for GAP specificity (Li et al., 1997). These predicted unfavorable interactions are consistent with the lack of RhoGAP activity in β2-chimaerin (Caloca et al., 2003). The replacement of the two acidic residues in Rho by two Ala residues in Rac negates these inhibitory interactions.

The observed β2-chimaerin structure appears to be inactive for catalysis in two respects. First, Pro21 and Pro22 directly occlude the Rac binding site (Figure 7A). Second, the αF′ helix appears to be locked in the unliganded conformation (Figure 7B). The liganded conformation of p50RhoGAP suggests the likely conformation of the β2-chimaerin RacGAP domain in complex with substrate. The liganded complex predicts a movement of the helix by ~6 Å in order to make contact with Rac. This structural change would lead to carbon-carbon contacts as close as 3.1 Å between Pro21 and Ser440 of the αF′ helix. Both of these inhibitory features could be relieved by a conformational change moving Pro21 and 22 out of their observed positions. However, the diPro unit is structurally rigid, the local environment in the Rac binding cleft is conformationally restrictive, and it is not apparent how such a structural change could occur without moving the residues that connect the diPro unit to the rest of β2-chimaerin. The next two residues in sequence, Ile23 and Trp24, are wedged between the C1 and RacGAP domain, and the N terminus is thereby anchored to both domains via extensive hydrophobic interactions. It appears that these interactions would need to be broken in order to free the diPro motif to move out of the GAP active site. Indeed, mutants that destabilize that inactive conformation are remarkably potent as RacGAPs as they reduce Rac-GTP levels in cells growing in 10% serum (Figure 5) as well as in response to EGF (H. Wang et al., unpublished).

Lipid Activation of β2-Chimaerin

Two central observations in this study allow us to propose a mechanism for the acidic phospholipid-dependent GAP activation of β2-chimaerin. First, the membrane penetrating and phorbol ester binding sites on β2-chimaerin are occluded by intramolecular interac-

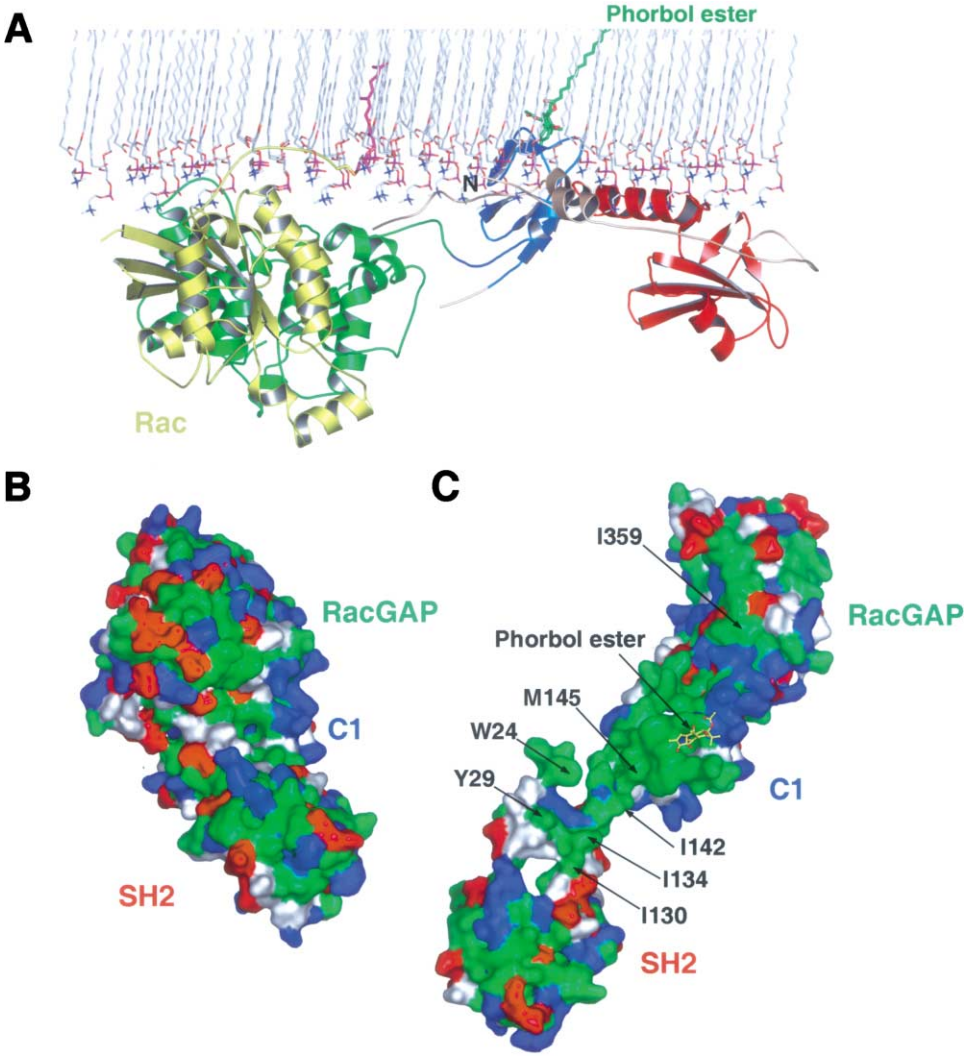

Figure 6. Membrane Interactions of β2-Chimaerin

(A) Model for membrane-docked, active β2-chimaerin, with domains colored as in Figure 1. The geranylgeranyl group is taken from the structure of Rac (yellow) bound to its guanine nucleotide dissociation inhibitor.

(B) Molecular surface of inactive β2-chimaerin. Hydrophobic surface is colored green, basic blue, acidic red, and uncharged polar white.

(C) Molecular surface of the model of the active, membrane bound β2-chimaerin, colored as in (B) and view looking directly out of the membrane.

tions with four separate regions of the protein. As described above, this implies that membrane engagement leads to a very large conformational change collapsing the interdomain interactions seen in the inactive state. Second, the Rac binding site on β2-chimaerin is occluded. Rac binding requires the removal of the N-ter-

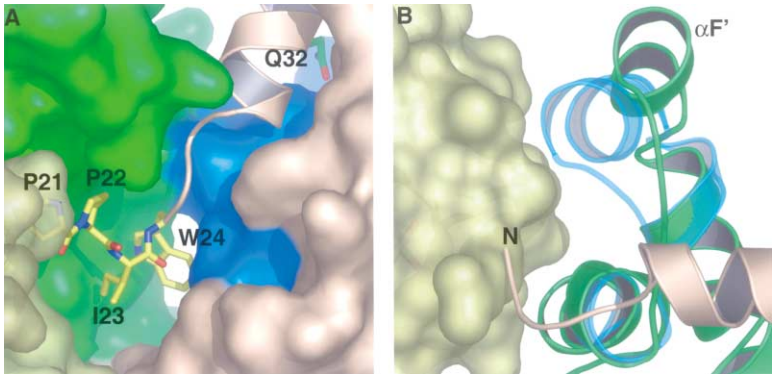

Figure 7. Autoinhibition and Activation of the RacGAP Domain

(A) Pro21 and Pro22 (yellow stick model) of β2-chimaerin, overlaid on the docked structure of Rac (translucent surface and model).

(B) The αF′ helix in the observed conformation (green) and predicted active conformation (cyan and translucent), with the N-terminal region in gray.

minal region from the RacGAP domain active site. The N-terminal segment is tightly anchored by the C1 and RacGAP domains, and it participates directly in the occlusion of the phospholipid binding site. We propose an activation model in which acidic phospholipid membranes compete with intramolecular interactions for binding to the C1 domain (Figure 6A). When the former bind, the latter interactions are disrupted. The disruption of these intramolecular interactions allows the N terminus sufficient flexibility to leave the RacGAP active site, removes steric inhibition of Rac binding, and permits the αF′ helix to adopt the active conformation (Figure 7B).

Implications for PKC and Other C1 Domain Proteins

Most biochemical investigation of phorbol ester and diacylglycerol-activated proteins has focused on the PKCs, which are ubiquitous in mammalian cell biology. Within the PKCs, the conventional isozymes (α, βI, βII, γ) have been the most thoroughly studied (Newton and Johnson, 1998). Conventional PKCs (cPKCs) contain an N-terminal pseudosubstrate region, two phorbol ester and diacylglycerol binding C1 domains, a Ca^{2+} binding C2 domain, and a protein kinase catalytic domain (Newton and Johnson, 1998). The novel PKCs (nPKCs; δ, ε, θ, η) are similar, except that they contain a C2 domain that does not bind Ca^{2+}. The structures of PKC C1 and C2 domains have been determined, but no structure of an intact PKC is available (Hurley, 2003). The cPKCs are potently activated in vitro and in vivo by phorbol esters or diacylglycerol in the presence of phospholipids. Like β2-chimaerin, L-phosphatidylserine is the preferred activating lipid (Newton and Johnson, 1998).

Activating lipids produce a large conformational change in cPKCs as judged by susceptibility to limited proteolysis (Orr et al., 1992). The N-terminal pseudosubstrate sequence functions as an autoinhibitory domain. The conformational change leads to the ejection of the N-terminal pseudosubstrate region from the active site of the catalytic domain and thence to enzyme activation (Orr and Newton, 1994). We now find from the present structure that β2-chimaerin, like the PKCs, has an N-terminal autoinhibitory region, albeit not one that has any relationship to the sequence of the substrate protein, Rac.

The cPKCs and nPKCs contain two C1 domains, and there is ample evidence that they have nonequivalent roles. The reason for the evolution of tandem C1 domains in PKCs has been a longstanding question. In PKCδ, the C1B domain is primarily responsible for translocation (Szallasi et al., 1996), implying that the C1A might be more buried. In PKCγ, both C1 domains are thought to be exposed (Ananthanarayanan et al., 2003). Conflicting reports suggest that in PKCα (Bogi et al., 1999), both C1 domains are equally important for translocation, yet the C1A domain is more buried (Ananthanarayanan et al., 2003). It is likely that the PKCs are translocated primarily by the more accessible of their two C1 domains. β2-chimaerin is a relatively inefficient translocator compared to the PKCs, and it is an example of a buried C1 domain. β2-chimaerin might be considered a primitive C1 domain in which both the activation and translocation functionalities reside in a single domain. In the more sophisticated PKCs, the functions appear to have diverged, with each C1 domain specialized for a unique purpose. The presence of a relatively accessible C1 domain enhances sensitivity to low levels of diacylglycerol, while the more buried C1 domain is required for allosteric activation.

The activating conformational change in β2-chimaerin not only exposes the hydrophobic membrane binding surface of the C1 domain, but it also exposes hydrophobic surfaces in the four other regions of β2-chimaerin that were formerly wrapped around the C1 domain. In order to avoid exposing a large amount of hydrophobic surface area to solvent, these regions must reassociate with each other, or with the membrane. The latter seems more likely, in that specific packing arrangements need not be fulfilled. It has been shown that the pseudosubstrate region of PKC is capable of binding to membranes (Mosior and McLaughlin, 1991), and the presence of this region directly contributes to stabilizing the association of PKC with cell membranes in vivo (Oancea and Meyer, 1998). By the same token, the hydrophobic faces of linker regions freed by an activating conformational change in β2-chimaerin are also likely to stabilize membrane association.

Experimental Procedures

Expression and Purification of β2-Chimaerin

β2-chimaerin was expressed as a glutathione S-transferase (GST) fusion protein in Sf9 cells using a baculovirus vector (Caloca et al., 1997). Sf9 cells were infected in roller bottles and grown on 245 mm nontreated square bioassay dishes (Corning). The plates were incubated at 27°C for 72 hr. The cells were harvested by centrifugation at 2000 rpm, washed with phosphate-buffered saline (PBS), and frozen at −80°C. Cells were lysed by homogenization in 20 mM Tris-HCl (pH 7.4), 100 mM NaCl, 1% (w/v) octylglucoside, 1 mM PMSF, 2 mM DTT, 1 mM EDTA, 1 mM NaF, 1 mM benzamidine, 10 mM β-glycerolphosphate, and 2 mM sodium pyrophosphate. The cell lysate was centrifuged at 100,000 × g for 30 min at 4°C. The supernatant was mixed with glutathione-sepharose 4B beads (Amersham-Pharmacia). The GST-β2-chimaerin fusion protein was cleaved by incubating the beads with thrombin at 4°C overnight. The cleaved β2-chimaerin was eluted in 20 mM Tris-HCl (pH 7.4), 100 mM NaCl, 1 mM EDTA, 5 mM DTT, 1 mM benzamidine, and 1 mM PMSF. The protein was further purified with a phenyl sepharose column (Amersham-Pharmacia) using a 2 M to 0 mM NaCl gradient. The peak fractions were judged to be at least 99% pure by SDS-PAGE. The protein was then concentrated to approximately 80 mg/ml, in 20 mM Tris-HCl (pH 7.4), 300 mM NaCl, 1 mM EDTA, 5 mM DTT, and 1 mM benzamidine, and stored at 4°C.

Crystallization and Data Collection

Crystals were obtained at 4°C using the hanging drop method by mixing 80 mg/ml protein in storage buffer with an equal volume of a reservoir solution containing 50 mM Na/K phosphate (pH 6.8) and 0.5%–1.0% ethanol (200 proof). Crystals appeared in 48 hr and typically reached dimensions of 1.0 mm × 0.3 mm × 0.3 mm in two weeks. The crystals belong to the hexagonal space group $P6_122$ with one molecule per asymmetric unit. Unit cell dimensions are a = b = 131.09 Å and c = 288.75 Å. The solvent content of the crystal is 81%. Before data collection, crystals were cryoprotected in reservoir solution supplemented with glycerol (up to 45%). After 10 min of soaking, crystals were mounted on cryoloops (Hampton, Riverside, California) and were frozen in liquid propane.

Xenon-derivatized crystals were prepared in an Xcell pressure chamber (Oxford Cryosystems) using a xenon pressure of 20 bar for 3.5 min, after depressurization, crystals were immediately flash-frozen in propane (Soltis et al., 1997). The native data set was collected at the National Synchrotron Light Source (NSLS) X25 beamline using a charge-coupled device (CCD) detector at 95 K. The

derivative data set was collected at Advanced Proton Source (APS) SER-CAT beamline at the Zn edge in order to maximize native Zn anomalous scattering. Images were indexed and integrated with the program DENZO, and data were scaled using SCALEPACK, HKL Research (Otwinowski and Minor, 1997).

Structure Solution and Refinement

Phases were calculated from the Xe SAD dataset to 3.8 Å in SOLVE (Terwilliger and Berendzen, 1999). Three heavy atom sites were found in the asymmetric unit. Two of the sites coincided with the expected positions of Zn^{2+} ions in the C1 domain, and confirmed native scatterers based on their presence in a crossphased anomalous difference Fourier syntheses based on native data. The phases were extended to 3.2 Å and the map was solvent-flattened in RESOLVE (Terwilliger, 2000). The domains of β2-chimaerin were located by molecular replacement using Molrep. The SH2 domain, C1 domain, and RhoGAP domain were located in the electron density using pdb models 1jyu, 1ptr, and 1f7c as search models in Molrep, respectively. The rest of the model including the linkers between the domains and the amino terminus were built in the model building program O (Jones et al., 1991). Once the initial model building was completed, the structure was refined using CNS (Brunger et al., 1998) at 3.2 Å using positional and torsion angle dynamics and B factor refinement with a maximum likelihood target. Residues 1–20 and 162–208 of the molecule were excluded from the model due to their disorder. The model has a working R factor of 24.8% and a free R factor of 29.0%. None of the nonglycine residues are in the disallowed region of the Ramachandran plot.

Mutagenesis and Translocation Assays

Single mutants for β2-chimaerin were generated using the QuikChange II XL site-directed mutagenesis kit (Stratagene, La Jolla, California). pEGFP-β2-chimaerin (Caloca et al., 2001) was used as a template. For translocation studies, COS-1 cells were cultured in Dulbecco's modified Eagle's medium supplemented with 10% fetal bovine serum, 100 units/ml penicillin, and 100 μg/ml streptomycin at 37°C in a humidified 5% CO2 atmosphere. pEGFP vectors encoding for wild-type β2-chimaerin (Caloca et al., 1999) or β2-chimaerin mutants were transfected into COS-1 cells in 6-well plates using FuGENE6 (Roche Molecular Biochemicals). Forty eight hours after transfection, cells were treated with different concentrations of PMA for 20 min. Experiments were performed in the presence of the PKC inhibitor GF 109203X (5 μM), added 30 min before and during the incubation with PMA, as we have previously described (Caloca et al., 1997). Cells were harvested into lysis buffer (50 mM Tris-HCl, pH 7.4, 5 mM EGTA, 5 μg/ml 4-(2-aminoethyl)-benzenesulfonyl fluoride, 5 μg/ml leupeptin, 5 μg/ml aprotinin, and 1 μg/ml pepstatin A) and lysed by sonication. Separation of cytosolic (soluble) and particulate fractions was performed by ultracentrifugation as described previously (Caloca et al., 1997, 1999). Equal amounts of protein (10 μg) for each fraction were subjected to SDS-polyacrylamide gel electrophoresis and transferred to PVDF membranes that were immunostained with either an anti-GFP antibody (1:5,000; Covance Inc. Princeton, New Jersey) or an anti-PKCα antibody (1:3,000; Upstate Biotechnology Inc., Lake Placid, New York). Densitometry analysis was performed using a AlphaImager™ system (Alpha Innotech).

Determination of Rac-GTP Levels

A pull-down assay was used to isolate Rac-GTP by binding to the p21 binding domain of PAK1 (Benard et al., 1999). Cells were lysed in a buffer containing 8 μg of GST-p21 binding domain protein, 20 mM Tris-HCl, pH 7.5, 1 mM dithiothreitol, 5 mM $MgCl_2$, 150 mM NaCl, 0.5% Nonidet P-40, 5 mM β-glycerophosphate, and a protease inhibitor cocktail (Sigma). Lysates were centrifuged at 14,000 × g (4°C, 10 min) and then incubated with glutathione-Sepharose 4B beads (4°C, 1 hr). After extensive washing, the beads were boiled in loading buffer. Samples were run in a 12% SDS-polyacrylamide gel and transferred to a PVDF membrane for Western blot analysis using a monoclonal anti-Rac antibody (Upstate Biotechnology).

Acknowledgments

We thank A. Newton, S. McLaughlin, T. Pawson, S. Hubbard, and W. Smith for discussions and comments on the manuscript and acknowledge the use of synchrotron facilities at the NSLS beamline X25, the APS SER-CAT and SBC-CAT beamlines, and the ALS. M.G.K. acknowledges the support from NIH grant RO1-CA74197. Use of the Advanced Photon Source was supported by the U.S. Department of Energy, Basic Energy Sciences, Office of Science, under Contract No.W-31-109-Eng-38.

Received: May 14, 2004
Revised: August 25, 2004
Accepted: October 15, 2004
Published: October 28, 2004

References

Ahmed, S., Kozma, R., Monfries, C., Hall, C., Lim, H.H., Smith, P., and Lim, L. (1990). Human brain N-chimaerin cDNA encodes a novel phorbol ester receptor. Biochem. J. *272*, 767–773.

Ahmed, S., Lee, J., Kozma, R., Best, A., Monfries, C., and Lim, L. (1993). A novel functional target for tumor-promoting phorbol esters and lysophosphatidic acid–the P21rac-Gtpase activating protein N-chimaerin. J. Biol. Chem. *268*, 10709–10712.

Ananthanarayanan, B., Stahelin, R.V., Digman, M.A., and Cho, W.H. (2003). Activation mechanisms of conventional protein kinase C isoforms are determined by the ligand affinity and conformational flexibility of their C1 domains. J. Biol. Chem. *278*, 46886–46894.

Areces, L.B., Kazanietz, M.G., and Blumberg, P.M. (1994). Close similarity of baculovirus-expressed N-chimaerin and protein-kinase C-alpha as phorbol ester receptors. J. Biol. Chem. *269*, 19553–19558.

Barrett, T., Xiao, B., Dodson, E.J., Dodson, G., Ludbrook, S.B., Nurmahomed, K., Gamblin, S.J., Musacchio, A., Smerdon, S.J., and Eccleston, J.F. (1997). The structure of the GTPase-activating domain from p50rhoGAP. Nature *385*, 458–461.

Benard, V., Bohl, B.P., and Bokoch, G.M. (1999). Characterization of Rac and Cdc42 activation in chemoattractant-stimulated human neutrophils using a novel assay for active GTPases. J. Biol. Chem. *274*, 13198–13204.

Betz, A., Ashery, U., Rickmann, M., Augustin, I., Neher, E., Sudhof, T.C., Rettig, J., and Brose, N. (1998). Munc13-1 is a presynaptic phorbol ester receptor that enhances neurotransmitter release. Neuron *21*, 123–136.

Bishop, A.L., and Hall, A. (2000). Rho GTPases and their effector proteins. Biochem. J. *348*, 241–255.

Bogi, K., Lorenzo, P.S., Acs, P., Szallasi, Z., Wagner, G.S., and Blumberg, P.M. (1999). Comparison of the roles of the C1a and C1b domains of protein kinase C alpha in ligand induced translocation in NIH 3T3 cells. FEBS Lett. *456*, 27–30.

Brose, N., and Rosenmund, C. (2002). Move over protein kinase C, you've got company: Alternative cellular effectors of diacylglycerol and phorbol esters. J. Cell Sci. *115*, 4399–4411.

Brunger, A.T., Adams, P.D., Clore, G.M., DeLano, W.L., Gros, P., Grosse-Kunstleve, R.W., Jiang, J.S., Kuszewski, J., Nilges, M., Pannu, N.S., et al. (1998). Crystallography & NMR system: A new software suite for macromolecular structure determination. Acta Crystallogr. D *54*, 905–921.

Caloca, M.J., Fernandez, N., Lewin, N.E., Ching, D.X., Modali, R., Blumberg, P.M., and Kazanietz, M.G. (1997). β2-chimaerin is a high affinity receptor for the phorbol ester tumor promoters. J. Biol. Chem. *272*, 26488–26496.

Caloca, M.J., Garcia-Bermejo, M.L., Blumberg, P.M., Lewin, N.E., Kremmer, E., Mischak, H., Wang, S.M., Nacro, K., Bienfait, B., Marquez, V.E., and Kazanietz, M.G. (1999). β2-chimaerin is a novel target for diacylglycerol: Binding properties and changes in subcellular localization mediated by ligand binding to its C1 domain. Proc. Natl. Acad. Sci. USA *96*, 11854–11859.

Caloca, M.J., Wang, H.B., Delemos, A., Wang, S.M., and Kazanietz, M.G. (2001). Phorbol esters and related analogs regulate the subcellular localization of β2-chimaerin, a non-protein kinase C phorbol ester receptor. J. Biol. Chem. *276*, 18303–18312.

Caloca, M.J., Wang, H.B., and Kazanietz, M.G. (2003). Characteriza-

tion of the Rac-GAP (Rac-GTPase-activating protein) activity of β2-chimaerin, a 'non-protein kinase C' phorbol ester receptor. Biochem. J. *375*, 313–321.

Ebinu, J.O., Bottorff, D.A., Chan, E.Y.W., Stang, S.L., Dunn, R.J., and Stone, J.C. (1998). RasGRP, a Ras guanyl nucleotide-releasing protein with calcium- and diacylglycerol-binding motifs. Science *280*, 1082–1086.

Hall, C., Monfries, C., Smith, P., Lim, H.H., Kozma, R., Ahmed, S., Vanniasingham, V., Leung, T., and Lim, L. (1990). Novel human-brain Cdna-encoding a 34,000 Mr protein N-chimaerin, related to both the regulatory domain of protein kinase-C and Bcr, the product of the breakpoint cluster region gene. J. Mol. Biol. *211*, 11–16.

Hommel, U., Zurini, M., and Luyten, M. (1994). Solution structure of a cysteine-rich domain of rat protein-kinase-C. Nat. Struct. Biol. *1*, 383–387.

Hu, J.J., Liu, J., Ghirlando, R., Saltiel, A.R., and Hubbard, S.R. (2003). Structural basis for recruitment of the adaptor protein APS to the activated insulin receptor. Mol. Cell *12*, 1379–1389.

Hurley, J.H. (2003). Structural analysis of protein kinase C: an introduction. Methods Mol. Biol. *233*, 289–290.

Hurley, J.H., and Misra, S. (2000). Signaling and subcellular targeting by membrane-binding domains. Annu. Rev. Biophys. Biomol. Struct. *29*, 49–79.

Hurley, J.H., and Meyer, T. (2001). Subcellular targeting by membrane lipids. Curr. Opin. Cell Biol. *13*, 146–152.

Hurley, J.H., Newton, A.C., Parker, P.J., Blumberg, P.M., and Nishizuka, Y. (1997). Taxonomy and function of C1 protein kinase C homology domains. Protein Sci. *6*, 477–480.

Jones, T.A., Zou, J.Y., Cowan, S.W., and Kjeldgaard, M. (1991). Improved methods for building protein models in electron-density maps and the location of errors in these models. Acta Crystallograp. A *47*, 110–119.

Kazanietz, M.G., Barchi, J.J., Omichinski, J.G., and Blumberg, P.M. (1995a). Low-affinity finding of phorbol esters to protein-kinase-C and its recombinant cysteine-rich region in the absence of phospholipids. J. Biol. Chem. *270*, 14679–14684.

Kazanietz, M.G., Wang, S., Milne, G.W.A., Lewin, N.E., Liu, H.L., and Blumberg, P.M. (1995b). Residues in the 2nd cysteine-rich region of protein-kinase-C-delta relevant to phorbol ester binding as revealed by site-directed mutagenesis. J. Biol. Chem. *270*, 21852–21859.

Kikkawa, U., Kishimoto, A., and Nishizuka, Y. (1989). The protein kinase-C family—Heterogeneity and its implications. Annu. Rev. Biochem. *58*, 31–44.

Leung, T., How, B.E., Manser, E., and Lim, L. (1994). Cerebellar β2-chimaerin, a Gtpase-activating protein for P21 Ras-related Rac is specifically expressed in granule cells and has a unique N-terminal Sh2 domain. J. Biol. Chem. *269*, 12888–12892.

Li, R., Zhang, B.L., and Zheng, Y. (1997). Structural determinants required for the interaction between rho GTPase and the GTPase-activating domain of p190. J. Biol. Chem. *272*, 32830–32835.

Medkova, M., and Cho, W.H. (1999). Interplay of C1 and C2 domains of protein kinase C-alpha in its membrane binding and activation. J. Biol. Chem. *274*, 19852–19861.

Mellor, H., and Parker, P.J. (1998). The extended protein kinase C superfamily. Biochem. J. *332*, 281–292.

Mosior, M., and McLaughlin, S. (1991). Peptides that mimic the pseudosubstrate region of protein- kinase-C bind to acidic lipids in membranes. Biophys. J. *60*, 149–159.

Musacchio, A., Cantley, L.C., and Harrison, S.C. (1996). Crystal structure of the breakpoint cluster region homology domain from phosphoinositide 3-kinase p85 alpha subunit. Proc. Natl. Acad. Sci. USA *93*, 14373–14378.

Nassar, N., Hoffman, G.R., Manor, D., Clardy, J.C., and Cerione, R.A. (1998). Structures of Cdc42 bound to the active and catalytically compromised forms of Cdc42GAP. Nat. Struct. Biol. *5*, 1047–1052.

Newton, A.C., and Johnson, J.J. (1998). Protein kinase C: a paradigm for regulation of protein function by two membrane-targeting modules. Biochim. Biophys. Acta *1376*, 155–172.

Nishizuka, Y. (1988). The molecular heterogeneity of protein kinase-C and its implications for cellular-regulation. Nature *334*, 661–665.

Nishizuka, Y. (1992). Intracellular signaling by hydrolysis of phospholipids and activation of protein-kinase-C. Science *258*, 607–614.

Nishizuka, Y. (1995). Protein kinases.5. Protein-kinase-C and lipid signaling for sustained cellular-responses. FASEB J. *9*, 484–496.

Oancea, E., and Meyer, T. (1998). Protein kinase C as a molecular machine for decoding calcium and diacylglycerol signals. Cell *95*, 307–318.

Ono, Y., Fujii, T., Igarashi, K., Kuno, T., Tanaka, C., Kikkawa, U., and Nishizuka, Y. (1989). Phorbol ester binding to protein kinase-C requires a cysteine-rich zinc-finger-like sequence. Proc. Natl. Acad. Sci. USA *86*, 4868–4871.

Orr, J.W., and Newton, A.C. (1994). Intrapeptide regulation of protein-kinase-C. J. Biol. Chem. *269*, 8383–8387.

Orr, J.W., Keranen, L.M., and Newton, A.C. (1992). Reversible exposure of the pseudosubstrate domain of protein-kinase-C by phosphatidylserine and diacylglycerol. J. Biol. Chem. *267*, 15263–15266.

Otwinowski, Z., and Minor, W. (1997). Processing of X-ray diffraction data collected in oscillation mode. In Macromolecular Crystallography, Pt A, pp. 307–326.

Rhee, J.S., Betz, A., Pyott, S., Reim, K., Varoqueaux, F., Augustin, I., Hesse, D., Sudhof, T.C., Takahashi, M., Rosenmund, C., and Brose, N. (2002). Beta phorbol ester- and diacylglycerol-induced augmentation of transmitter release is mediated by Munc13s and not by PKCs. Cell *108*, 121–133.

Rittinger, K., Walker, P.A., Eccleston, J.F., Nurmahomed, K., Owen, D., Laue, E., Gamblin, S.J., and Smerdon, S.J. (1997a). Crystal structure of a small G protein in complex with the GTPase-activating protein rhoGAP. Nature *388*, 693–697.

Rittinger, K., Walker, P.A., Eccleston, J.F., Smerdon, S.J., and Gamblin, S.J. (1997b). Structure at 1.65 angstrom of RhoA and its GTPase-activating protein in complex with a transition-state analogue. Nature *389*, 758–762.

Ron, D., and Kazanietz, M.G. (1999). New insights into the regulation of protein kinase C and novel phorbol ester receptors. FASEB J. *13*, 1658–1676.

Scheffzek, K., Lautwein, A., Kabsch, W., Ahmadian, M.R., and Wittinghofer, A. (1996). Crystal structure of the GTPase-activating domain of human p120GAP and implications for the interaction with Ras. Nature *384*, 591–596.

Sicheri, F., Moarefi, I., and Kuriyan, J. (1997). Crystal structure of the Src family tyrosine kinase Hck. Nature *385*, 602–609.

Slater, S.J., Milano, S.K., Stagliano, B.A., Gergich, K.J., Ho, C.J., Mazurek, A., Taddeo, F.J., Kelly, M.B., Yeager, M.D., and Stubbs, C.D. (1999). Synergistic activation of protein kinase C alpha, -beta I, and -gamma isoforms induced by diacylglycerol and phorbol ester: Roles of membrane association and activating conformational changes. Biochemistry *38*, 3804–3815.

Soltis, S.M., Stowell, M.H.B., Wiener, M.C., Phillips, G.N., and Rees, D.C. (1997). Successful flash-cooling of xenon-derivatized myoglobin crystals. J. Appl. Crystallogr. *30*, 190–194.

Szallasi, Z., Bogi, K., Gohari, S., Biro, T., Acs, P., and Blumberg, P.M. (1996). Non-equivalent roles for the first and second zinc fingers of protein kinase C delta—Effect of their mutation on phorbol ester-induced translocation in NIH 3T3 cells. J. Biol. Chem. *271*, 18299–18301.

Terwilliger, T.C. (2000). Maximum-likelihood density modification. Acta Crystallogr. D *56*, 965–972.

Terwilliger, T.C., and Berendzen, J. (1999). Automated MAD and MIR structure solution. Acta Crystallogr. D *55*, 849–861.

Tognon, C.E., Kirk, H.E., Passmore, L.A., Whitehead, I.P., Der, C.J., and Kay, R.J. (1998). Regulation of RasGRP via a phorbol ester-responsive C1 domain. Mol. Cell. Biol. *18*, 6995–7008.

Wurtele, M., Wolf, E., Pederson, K.J., Buchwald, G., Ahmadian, M.R., Barbieri, J.T., and Wittinghofer, A. (2001). How the Pseudomonas aeruginosa ExoS toxin downregulates Rac. Nat. Struct. Biol. *8*, 23–26.

Xu, R.X., Pawelczyk, T., Xia, T.H., and Brown, S.C. (1997a). NMR structure of a protein kinase C-gamma phorbol-binding domain and study of protein-lipid micelle interactions. Biochemistry *36*, 10709–10717.

Xu, W.Q., Harrison, S.C., and Eck, M.J. (1997b). Three-dimensional structure of the tyrosine kinase c-Src. Nature *385*, 595–602.

Yuan, S.X., Miller, D.W., Barnett, G.H., Hahn, J.F., and Williams, B.R.G. (1995). Identification and characterization of human β2-chimaerin—Association with malignant transformation in astrocytoma. Cancer Res. *55*, 3456–3461.

Zhang, G.G., Kazanietz, M.G., Blumberg, P.M., and Hurley, J.H. (1995). Crystal-structure of the Cys2 activator-binding domain of protein-kinase C-delta in complex with phorbol ester. Cell *81*, 917–924.

Accession numbers

Coordinates have been deposited in the Protein Data Bank with accession code 1XA6.